Wall-contact sliding control strategy for a 2D caged quadrotor

Pu Bai[2,1], Bruno Guerreiro[1], Rita Cunha[1], Przemyslaw Kornatowski[2], Dario Floreano[2], and Carlos Silvestre[3,1]

[1]Institute for Systems and Robotics (ISR/IST), LARSYS,
Instituto Superior Técnico, Universidade de Lisboa, Portugal
[2] Laboratory of Intelligent Systems, École Polytechnique Fédérale de Lausanne, Switzerland
[3] Faculty of Science and Technology, University of Macau, Taipa, Macau SAR, China

Abstract: This paper addresses the trajectory tracking problem of a 2D caged flying robot in contact with a wall. To simplify the contact problem, the models are constructed on a vertical two dimensional plane, and our objective is to let the quadrotor hover or move along the wall with arbitrary velocity and attitude. The control law is derived using Lyapunov stability theory, applying backstepping techniques to achieve exponential stability under mild assumptions. To overcome the unknown friction force between robot and wall, we design estimators for the friction coefficient, which include a projection operator that provides an upper bound for the obtained estimates. Realistic simulation results are provided to validate the proposed methodology.

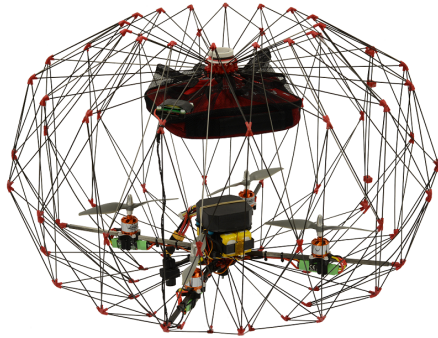**Keywords:** trajectory tracking, contact, backstepping, estimation

Fig. 1 The cage: a foldable cargo delivery drone with protective structure [2].

1. INTRODUCTION

Unmanned Aerial Vehicles (UAVs) are known for their safety, low weight, high flexibility, and agility, thus they have been widely adopted in search and rescue, topographic mapping, precision agriculture, among other commercial and military applications. The ongoing development of more advanced sensors, actuators, and algorithms opens up new possible applications, as mentioned in [1]. Among them, drone delivery gets attention both from the scientific perspective and for commercial purposes.

The caged drone [2], [3], shown in Fig. 1, is a delivery quadcopter that adopts foldable structure to optimize the space utilization. The drone is surrounded by 3D printed holders and carbon rods to protect electronics and cargo. Thanks to such mechanical design, the cage is able to attempt new flying strategies and applications that classical drones are not able to conduct, such as indoor flying or infrastructure close inspections.

Even equipped with a protective structure, the research interests of drone indoor flying are to avoid obstacles, typically using optical flow [4] or visual SLAM [5] to evade obstructions. The reason why avoiding obstacles is preferable is due to the fragility of the flying robots, and the difficulty of stability recovery after impact. This paper, on the contrary, addresses control problems that are needed in systems that learn from contact. There are quite a few works studying drone-environment interaction, where robotic arms are often considered as the media for quadrotor to interact with the world. A hierarchical control scheme and a sliding model controller were proposed to control the whole system in [6] and [7], respectively. On a different approach, the study presented in [8] explored how to make the tip of a rigid link attached on the top of a quadrotor slide on the ceiling. To overcome the situations when a quadrotor can be pulled towards walls, caused by low pressure area above the propellers when it tilts toward the wall, a novel quadrotor design and control was introduced in [9]. It is equipped with an extra horizontal propeller and a brush to maintain stability while sliding on the wall. Another ducted fan aerial robot is designed for moving vertically on the wall by tracking a desired signal and applying a desired constant force against the wall [10]. Researchers also attempted to put the quadrotor into an airframe to ensure safe physical interaction, and use hybrid model predictive control (MPC) to generate the control law [11]. A micro aerial vehicle equipped with a 3-axis gimbal protective frame is studied in [12]. The two independent systems design weakens the influence of collision to the inner system, guarantees it to be upright even after impact. Therefore, this flying robot is able to perform robust flying in cluttered environments without complex sensory systems.

Conversely to the above approaches, the strategy proposed in this paper aims at guaranteeing stability after collision, and maintaining contact with the wall if desired, enabling the use of collision information for per-

ception and navigation in unknown environments. In the proposed approach, the vehicle is controlled towards a desired orientation and in a planned path while keeping contact with obstacles, providing more flexibility when compared to an immutable attitude as described in [12].

The objective of this work is to design an algorithm that drives the quadcopter sliding on the wall by controlling its propellers, or equivalently, the thrust and torques generated by them. More specifically, we want the drone to track a trajectory next to the wall, consisting of desired position and velocity profiles, where the component perpendicular to the wall is zero. There are several potential applications using this strategy, among which the use of indoor flying robots to transport items between offices in a building is a good example. The protective cage, combined with a slow motion behavior, guarantees safety for people, property, and the vehicle itself, whereas the sliding flying capabilities allow the vehicle to fly along walls, floor, or ceiling to avoid other vehicles or obstacles, or enter another room by applying a thrust on the door to open it. Another application scenario, where a drone needs to deliver a parcel to a customer in a designated apartment within a building, having the capability of sliding along a surface, may enable the drone to briefly enter the apartment through a window to deliver its parcel.

For simplicity, the model of the caged quadrotor and its workspace are restricted in 2D space in this paper. A nonlinear control law is designed to solve its trajectory tracking problem by using backstepping techniques, assuming a known friction coefficient. Then, considering an unknown friction coefficient in the model, a two-stage estimator is applied to balance the friction, upper bounded by a designated value to prevent overflow. Therefore, the main contributions of this work are the 2D vehicle-wall model and two control laws that provide exponential stability guarantees, either when the friction coefficient is known or when it is unknown or changes through time.

This paper is structured as follows. Section 2 states the problem we want to solve, providing further motivation and the vehicle-wall model used throughout the paper. The control law design with the knowledge of friction and stability analysis are stated in Section 3, while the estimators are designed in Section 4 to overcome the unknown friction produced by the contact. Section 5 shows the simulation results of the designed control law. Finally, section 6 provides some concluding remarks.

2. PROBLEM STATEMENT

Building on the benefits of having a simple structure and actuation mechanism, together with a relatively low cost when compared with similar vehicles, quadrotors have been intensively studied as a platform for testing free flight strategies. Towards that end, numerous algorithms for sensor processing and vehicle maneuvering have emerged, namely, path planning, collision avoidance, trajectory tracking, flight stability, disturbance rejection, or signal delay problems. Compared to the popularity of quadrotor free flight control, vehicle-obstacle interaction is a relative unexplored topic. One possible reason is that quadcopters are usually vulnerable to contact, as they may briefly loose stability or even crash. Additionally, contact with obstacles during flight limits the motion of the vehicle and introduces more disturbances at the contact point or plane, which implies that algorithms tailored for free flight may not be directly applied to this problem. Recently, novel drone designs appear in an inexhaustible variety aiming at new applications. Some of them have protective structures or deformable shape to protect the functional parts. Therefore, contact flying is becoming more and more plausible.

This paper discusses the wall-vehicle 2D interactions of a quadrotor, surrounded by a circular cage. The objective is to design a control law for a 2D quadrotor, such that it always stays in contact with the wall, and follows a given trajectory consisting of 2D position, velocity, and tilting between the wall, allowing the quadrotor to move freely along the wall plane. Assume the quadrotor is flying against the wall, the 2D caged quadrotor dynamics in contact with the wall are described by

$$
\begin{cases}
\dot{\mathbf{p}} = \mathbf{v} & \text{(1a)} \\
\dot{\mathbf{v}} = -g\mathbf{e}_2 + \dfrac{u_1}{m}\cos\theta\,\mathbf{e}_2 - \dfrac{u_1\mu}{m}\sin\theta\,\mathbf{e}_2 & \text{(1b)} \\
\dot{\theta} = \omega & \text{(1c)} \\
\dot{\omega} = \dfrac{u_2 + u_1\mu\sin\theta\,r}{J} & \text{(1d)}
\end{cases}
$$

where $m, J \in \mathbb{R}$ are the mass and moment of inertia of the 2D quadrotor, respectively, $\mathbf{p}, \mathbf{v} \in \mathbb{R}^2$ represent the position and linear velocity, respectively, of the body frame $\{B\}$ with respect to the inertial frame $\{I\}$, expressed in $\{I\}$, $\mathbf{e}_i \in \mathbb{R}^2$ is the i-th vector of the canonical basis of a 2D space $\mathbb{R}^2$, i.e. $\mathbf{e}_1 = [1, 0]^T$, $\theta, \omega \in \mathbb{R}$ denote the attitude and angular velocity expressed in $\{B\}$, respectively, r is the radius of the quadrotor cage, u_1, $u_2 \in \mathbb{R}$ are the control thrust and torque to be designed. The friction coefficient μ at the contact point adopt a velocity-based model [13]

$$
\begin{aligned}
\mu = \mu_0 f(v_{rel}) =&\mu_0 \sin\Big\{ C\tan^{-1}\Big[Av_{rel} \\
&- E\Big(Av_{rel} - \tan^{-1}\left(Av_{rel} \right) \Big) \Big] \Big\}
\end{aligned}
\tag{2}
$$

where A, C, E are constants that define some properties of the contact plane, μ_0 represents the maximum static friction coefficient, and the relative motion between the quadrotor and the wall at the same point is given by $v_{rel} = \mathbf{e}_2^T v - r\omega$.

Fig. 2 shows the forces acting on caged quadcopter while moving vertically along the wall, where $\mathbf{F_G} = mg\mathbf{e}_2$ is the gravity, the reaction force cancels out the horizontal component of the thrust $\mathbf{T}$, preventing the drone
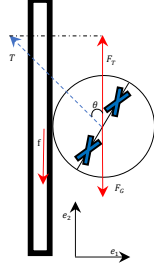
Fig. 2 The force analysis of a caged quadrotor when it is moving along the vertical axis of a wall.

leaving from the wall, while the resulting vertical component is given by $u_1 \cos\theta \mathbf{e}_2$. As the friction force is proportional to the horizontal component of the reaction force, we obtain the resulting friction $\mathbf{f} = -\mu u_1 \sin\theta \mathbf{e}_2$.

Given the friction coefficient $\mu \leq 1$, the desired trajectory, defined as $\{\mathbf{p}_d, \mathbf{v}_d, \theta_d \mid \mathbf{p}_d^T \mathbf{e}_2 = 0, \ \mathbf{v}_d^T \mathbf{e}_2 = 0, \ 0 \leq \theta_d \leq \frac{\pi}{4}\}$ defines the maximum region the drone is able to reach. A tighter upper bound of θ_d depends on how much thrust can be generated. Since the vehicle is not supposed to rotate vertically, the desired angular velocity is 0. Thus, the resulting error dynamics is given by

$$
\begin{cases}
\dot{\tilde{\mathbf{p}}} = \mathbf{v} - \mathbf{v}_d & \text{(3a)} \\
\dot{\tilde{\mathbf{v}}} = -g\mathbf{e}_2 + \dfrac{u_1}{m}\cos\theta\mathbf{e}_2 - \dfrac{u_1\mu}{m}\sin\theta\mathbf{e}_2 - \dot{\mathbf{v}}_d & \text{(3b)} \\
\dot{\tilde{\theta}} = \omega & \text{(3c)} \\
\dot{\omega} = \dfrac{u_2 + u_1\mu\sin\theta r}{J} & \text{(3d)}
\end{cases}
$$

where $\sim$ denotes the difference between the actual value and desired value, e.g., $\tilde{\mathbf{p}} = \mathbf{p} - \mathbf{p}_d$.

3. CONTROLLER DESIGN

Assuming full state feedback, one important source of uncertainty is the friction coefficient, that might be different in each wall of even within the same wall. Yet, for simplicity, we first assume in this section full knowledge of this coefficient, and in the next section we propose modifications in the control law to stabilize the system while estimating its value.

In order to fulfill the aforementioned objective, steer the the vehicle to fly along the wall, we want to design control laws for the actuation variables u_1 and u_2 such that the controlled system is stable for certain domain. The controller adopts a hierarchical backstepping fashion. The stability of the quadrotor state, as well as the estimation error, is achieved by proving the convergence of a Lyapunov-like function that summarizes each state.

Let the Lyapunov function including the error dynamics be

$$
V_1 = \frac{k_1}{2}\tilde{\mathbf{p}}^T\tilde{\mathbf{p}} + \frac{1}{2}(\tilde{\mathbf{v}} + k_2\tilde{\mathbf{p}})^T(\tilde{\mathbf{v}} + k_2\tilde{\mathbf{p}}) + \frac{k_3}{2}\tilde{\theta}^2
$$
$$
+ \frac{1}{2}(\omega + k_4\tilde{\theta})^2 \tag{4}
$$

Its derivative is given by

$$
\dot{V}_1 = k_1\tilde{\mathbf{p}}^T\tilde{\mathbf{v}} + (\tilde{\mathbf{v}} + k_2\tilde{\mathbf{p}})^T\Big(-g\mathbf{e}_2 + \frac{u_1}{m}\cos\theta\mathbf{e}_2
$$
$$
- \frac{u_1\mu}{m}\sin\theta\mathbf{e}_2 + k_2\tilde{\mathbf{v}}\Big) + k_3\tilde{\theta}\omega + (\omega + k_4\tilde{\theta})
$$
$$
\Big(\frac{u_2 + u_1\mu\sin\theta r}{J} + k_4\omega\Big)
$$

Assumption 1: The tilt angle θ always stays between 0 and $\frac{\pi}{4}$.

Assumption 2: The desired trajectory $\mathbf{p}_d$, $\mathbf{v}_d$, θ_d are smoothly differentiable individually.

Proposition 1: For system (3) that satisfies Assumption 1 and 2, with friction coefficient μ given, under our designed control law

$$
u_1 = \frac{m}{\cos\theta - \mu_0 f\sin\theta}\mathbf{e}_2^T(g\mathbf{e}_2 - k_p\tilde{\mathbf{p}} - k_v\tilde{\mathbf{v}} + \dot{\mathbf{v}}_d) \tag{5}
$$

$$
u_2 = J(-k_\omega\omega - k_\theta\tilde{\theta}) - u_1\mu_0 f\sin\theta r \tag{6}
$$

the quadrotor state error converges to $\mathbf{0}$ exponentially.

Proof: Assumption 1 guarantees that the dynamic model is valid during the trajectory, that is, the vehicle is always in contact with the wall. Assumption 2 ensures the proposed Lyapunov function is continuous differentiable. Substituting (5) and (6) into $\dot{V}_1$, it becomes

$$
\dot{V}_1 = -k_2k_p\tilde{\mathbf{p}}^T\tilde{\mathbf{p}} - (k_p - k_1 + k_2k_v - k_2^2)\tilde{\mathbf{p}}^T\tilde{\mathbf{v}}
$$
$$
- (k_v - k_2)\tilde{\mathbf{v}}^T\tilde{\mathbf{v}} - k_4k_\theta\tilde{\theta}^2 - (k_\omega - k_4)\omega^2
$$
$$
- (k_\theta - k_3 + k_4k_\omega - k_4^2)\tilde{\theta}\omega
$$

From here, V_1 and $\dot{V}_1$ can be written as compact forms $s^T M_1 s$ and $-s^T M_2 s$, respectively, where s is the vector of all the error states, M_1 and M_2 are symmetric matrices. There always exists positive numbers k_1, k_2, k_p, k_v, k_3, k_4, k_θ, k_ω, such that M_1 and M_2 are positive definite. Therefore, $\dot{V}_1 \leq -\frac{\lambda_{\min}(M_2)}{\lambda_{\max}(M_1)}V_1 \leq 0$, where λ are the eigenvalues of a square matrix. $\dot{V}_1$ is equal to 0 if and only if when all errors become 0. According to Lyapunov's theory, the origin is exponentially stable to the system with a least convergence rate $\frac{\lambda_{\min}(M_2)}{\lambda_{\max}(M_1)}$. ∎

4. CONTROLLER DESIGN WITH UNKNOWN FRICTION

In this section, we assume that the friction coefficient μ is unknown, but can be approximated by a function of the relative velocity, as described in Section 2. Although the contact between the cage and the wall is more complex when the quadrotor is moving along the wall, this simple assumption is comprehensive enough to solve our problem. With this assumption, we want to estimate the maximum static friction coefficient μ_0, which depends on the material and texture of both surfaces. Since it is a constant in the model, we are able to estimate its value and feedback to the controller. Yet, to avoid algebraic loop

in this coupled system, two estimators are required. We use $\hat{\mu}_1$ and $\hat{\mu}_2$ to represent the estimates of μ_0, and the differences between μ_0 and them are given by $\tilde{\mu}_1$ and $\tilde{\mu}_2$, respectively.

Now we attempt to add the estimation error term to the previous Lyapunov function:

$$V_2 = \frac{k_1}{2}\tilde{\mathbf{p}}^T\tilde{\mathbf{p}} + \frac{1}{2}(\tilde{\mathbf{v}} + k_2\tilde{\mathbf{p}})^T(\tilde{\mathbf{v}} + k_2\tilde{\mathbf{p}}) + \frac{k_3}{2}\tilde{\theta}^2 \\ + \frac{1}{2}(\omega + k_4\tilde{\theta})^2 + \frac{k_{e1}}{2}\tilde{\mu}_1^2 + \frac{k_{e2}}{2}\tilde{\mu}_2^2 \tag{7}$$

In a similar fashion, by letting the new control laws be given by

$$u_1 = \frac{m}{\cos\theta - \hat{\mu}_1 f \sin\theta}\mathbf{e}_2^T\left(g\mathbf{e}_2 - k_p\tilde{\mathbf{p}} - k_v\tilde{\mathbf{v}} + \dot{\mathbf{v}}_d\right) \tag{8}$$

$$u_2 = J(-k_\omega\omega - k_\theta\tilde{\theta}) - u_1\hat{\mu}_2 f\sin\theta r \tag{9}$$

the derivative becomes

$$\dot{V}_2 = \dot{V}_1 - \tilde{\mu}_1\left[k_{e1}\dot{\hat{\mu}}_1 + \frac{f\sin\theta}{\cos\theta - \hat{\mu}_1 f\sin\theta}(\tilde{\mathbf{v}} + k_2\tilde{\mathbf{p}})^T\right. \\ \left.(g\mathbf{e}_2 - k_p\tilde{\mathbf{p}} - k_v\tilde{\mathbf{v}} + \dot{\mathbf{v}}_d)\right] - \tilde{\mu}_2\left(k_{e2}\dot{\hat{\mu}}_2 - (\omega + k_4\theta)\right. \\ \left. u_1 f\sin\theta r\right)$$

When v_{ref} becomes 0, which means the quadcopter is hovering in contact with the wall, there is no friction between them under the velocity-based model. The values given by the estimators may not be near the true values, but they will still converge to some values. To avoid the divergence or a large value of the estimation affecting the performance of the controller, we use a saturation function to set an upper bound on the estimates. As the friction coefficient is naturally between 0 and 1, making the estimates never go beyond 1 is also reasonable. The bound is enforced by applying a projection function to the estimates, as defined below.

Definition 1 ([14]): A projection is defined as

$$\text{Proj}(x,\hat{s}) = x - \frac{\eta_1\eta_2}{2(\varsigma^2 + 2\varsigma B)^{n+1}B^2}\hat{s} \tag{10}$$

that meets the following properties:
1. $|\hat{s}| \leq B + \varsigma, \forall t \geq 0$
2. $\tilde{s}\text{Proj}(x,\hat{s}) \geq \tilde{s}\mu$
3. $\|\text{Proj}(x,\hat{s})\| \leq \|x\|(1 + (\frac{B+\varsigma}{B})^2) + \frac{(B+\varsigma)\epsilon}{2B^2}$
4. $\text{Proj}(x,\hat{s})$ is of class $\mathcal{C}^n$

where x is the original function to be projected, $B + \varsigma$ is the upper bound $\hat{s}$ is the estimate of a variable s, ς ϵ are any positive number, n is the parametric order of the system, which is 4 in this case. Two functions η_1 and η_2 are defined as

$$\eta_1 = \begin{cases} (\hat{s}^2 - B^2)^{n+1} & \text{if}(\hat{s}^2 - B^2) > 0 \\ 0 & \text{otherwise} \end{cases} \tag{11a}$$

$$\eta_2 = \hat{s}x + \sqrt{(\hat{s}x)^2 + \epsilon^2} \tag{11b}$$

Table 1 Parameters used in the simulation.

Parameter	k_2	k_4	k_p	k_v	k_θ	k_ω
Value	10	3	5	2	30	20
Parameter	k_{e1}	k_{e2}	B	ς	ϵ	n
Value	0.15	0.1	0.49	0.01	0.01	4

Proposition 2: Considering Assumptions 1 and 2, the vehicle-wall error dynamics (3) with control inputs given by (8) and (9), and estimation laws given by

$$\dot{\hat{\mu}}_{1,p} = \text{Proj}(\dot{\hat{\mu}}_1, \hat{\mu}_1) \tag{12}$$

$$\dot{\hat{\mu}}_{2,p} = \text{Proj}(\dot{\hat{\mu}}_1, \hat{\mu}_2) \tag{13}$$

where

$$\dot{\hat{\mu}}_1 = -\frac{f\sin\theta}{k_{e1}(\cos\theta - \hat{\mu}_1 f\sin\theta)}(\tilde{\mathbf{v}} + k_2\tilde{\mathbf{p}})^T \\ (g\mathbf{e}_2 - k_p\tilde{\mathbf{p}} - k_v\tilde{\mathbf{v}} + \dot{\mathbf{v}}_d) \tag{14}$$

$$\dot{\hat{\mu}}_2 = \frac{1}{k_{e2}}(\omega + k_4\theta)u_1 f\sin\theta r \tag{15}$$

,then the quadrotor state error converges exponentially fast to the origin.

Proof: By substituting (14) and (15) into $\dot{V}_2$, the extra non-negative terms are canceled out, resulting in $\dot{V}_2 = \dot{V}_1 \leq 0$. If we replace $\dot{\hat{\mu}}_1$ and $\dot{\hat{\mu}}_2$ by their projection functions in $\dot{V}_2$, we get

$$\dot{V}_{2,p} = \frac{d}{dt}\left[\frac{k_1}{2}\tilde{\mathbf{p}}^T\tilde{\mathbf{p}} + \frac{1}{2}(\tilde{\mathbf{v}} + k_2\tilde{\mathbf{p}})^T(\tilde{\mathbf{v}} + k_2\tilde{\mathbf{p}}) + \frac{k_3}{2}\tilde{\theta}^2\right. \\ \left. + \frac{1}{2}(\omega + k_4\tilde{\theta})^2\right] - k_{e1}\tilde{\mu}_1\dot{\hat{\mu}}_{1,p} - k_{e2}\tilde{\mu}_2\dot{\hat{\mu}}_{2,p}$$

From property 2 of Definition 1, $-k_{e1}\tilde{\mu}_1\dot{\hat{\mu}}_{1,p} \leq -k_{e1}\tilde{\mu}_1\dot{\hat{\mu}}_1$ and $-k_{e2}\tilde{\mu}_2\dot{\hat{\mu}}_{2,p} \leq -k_{e2}\tilde{\mu}_2\dot{\hat{\mu}}_2$. Therefore $\dot{V}_{2,p} \leq \dot{V}_2 = \dot{V}_1$ is negative definite. We conclude that the origin is exponentially stable for (3) with saturated estimations. ∎

5. SIMULATIONS

To verify the effectiveness of the control law, we tested several desired trajectories aiming at different applications. The vehicle initial state is generated randomly but not too far from desired initial state such that the initial error is not 0. The parameters used in the simulation are listed in Table 1. As an under-actuated system, the quadrotor position control is assisted by attitude control, which explains that attitude gains are greater than position gains. Other parameters are chosen such that the V_2 is a qualified Lyapunov function. The upper bound of the estimation is chosen to be 0.5 to observe the saturation function does work clearly. Noticing that k_1 and k_3 only appear in the Lyapunov function, not in the control law.

The first simulation considers a scenario where the vehicle is executing some tasks on the wall, like painting. As Fig. 3 shows, the desired height is a sinusoidal function and desired tilt is a constant. Thus, the quadrotor moves up and down repeatedly along the wall. We can see, after a brief transient, the vehicle is able to follow the desired trajectory, with a maximum error of 0.1 meters in position. Regarding the performance of the estimators, it can be seen that estimators converge to the true value of $\mu_0 = 0.3$ with an error of less than 0.05 in 3 seconds.

In the second simulation as shown in Fig. 5 and 6, the quadrotor is asked to follow a piecewise linear function such that it keeps a constant velocity in a period. In 0 $\sim$ 10s, the desired velocity is 0.8 m/s. During 10s $\sim$ 15s, it hovers at 8m height. Then it moves down with 0.6 m/s velocity and the desired tilt changes from 0.3 to 0.4. After 25s, the quadrotor flies up again with 0.5 m/s speed. The maximum static friction coefficient μ_0 is set to 0.4. We can clearly see that the trajectory is stabilized within 3 seconds after each transition. In Fig. 6, there are two cut-off when the estimates reach the bound 0.5, proving the effectiveness of the projection function. During the hovering time, estimators fail to converge to the correct value because the friction model suggests that there is no friction when there is no relative motion. Nevertheless, the failure of the estimation does not affect the flight control. The first estimator usually takes more time to converge than the second. One reason might be that like in position control, the estimation used in position part is slower than the attitude counterpart.

The third simulation focus on emulating the texture change of the contact plane during an exploration task. In this scenario, the quadrotor is slowly descending with 0.3 m/s velocity. After 20s, the maximum static friction coefficient changes from 0.1 to 0.3. Like the first two, the trajectory converge to the desired one in 3 seconds and has only slight surge after the coefficient change. As shown in Fig. 8, estimators are able to reveal the change of friction coefficient, and converge to the true value.

From above simulations, we conclude that the proposed control law executes all three tasks successfully and they end up with almost zero state error. Each time the trajectory experiences a non-smooth change, the estimations diverge because it violates Assumption 2. But each piecewise function meets the requirement individually. So the error converges to 0 eventually. Both estimators converge to the actual friction coefficient during normal flight. We can also observe that they are saturated when they reach the projection bound of 0.5, proving the projection function is compatible with the estimators.

6. CONCLUSION

In this work, we presented a 2D quadrotor control strategy that makes the caged drone follow a given trajectory along the wall. Additionally, we developed a two-stage estimator to compute the friction coefficient
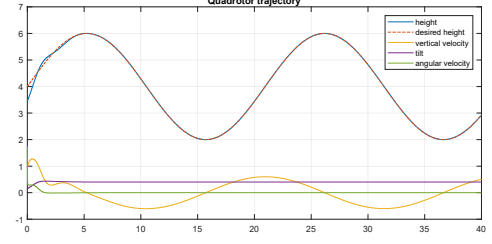

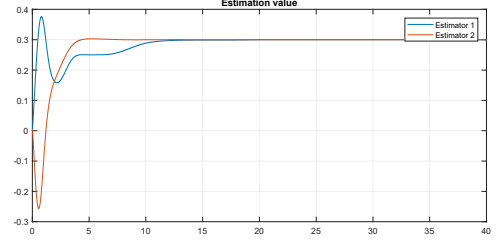Fig. 3 Time evolution of quadrotor state that tracks a sinusoidal trajectory.

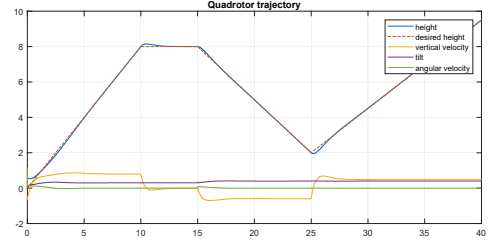Fig. 4 Both estimates converge to designed value.

Fig. 5 Time evolution of quadrotor state that tracks a piecewise constant velocity trajectory.
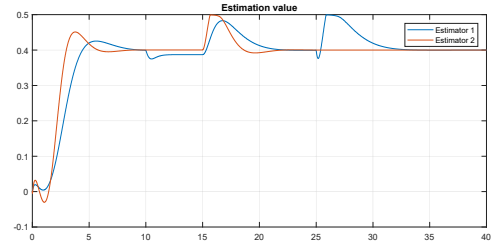

Fig. 6 Estimates converge to designed value during the flying time, and become different value during hovering.
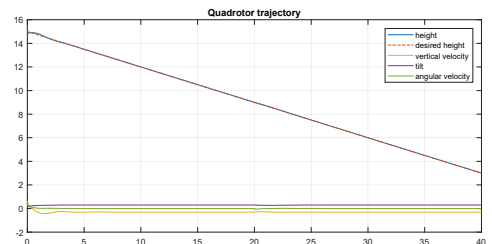

Fig. 7 Time evolution of quadrotor state that tracks a constant velocity trajectory .
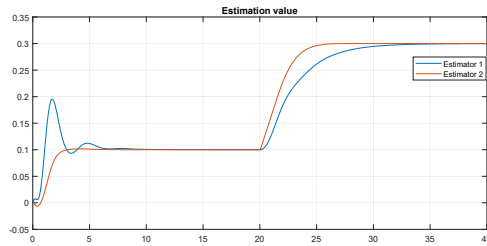
Fig. 8 Estimates experience a deviation after contact material changes.

between the vehicle and wall at the contact point, which is fed to the controller to generate a corresponding thrust. To avoid estimator saturation affecting the controller, we put an upper bound on estimators to suppress the overshoot. Our method is verified by simulations with various trajectories.

There are still theoretical and practical issues that need further research. Firstly, to ensure Assumption 1 is always satisfied, there should be a saturation operator to constrain the tilt angle by controlling the angular acceleration. Moreover, the presented modeling and controller design can be migrated to a 3D framework, so that it can be used in more applications and also experimentally tested.

7. ACKNOWLEDGMENTS

REFERENCES

[1] D. Floreano and R.J. Wood. Science, technology and the future of small autonomous drones. *Nature*, 521(7553):460–466, 2015.

[2] Przemyslaw Mariusz Kornatowski, Stefano Mintchev, and Dario Floreano. An origami-inspired cargo drone. In *IEEE/RSJ International Conference on Intelligent Robots and Systems*, 2017.

[3] *Dronistics*. Available at https://dronistics.epfl.ch.

[4] F. Expert and F. Ruffier. Flying over uneven moving terrain based on optic-flow cues without any need for reference frames or accelerometers. *Bioinspiration & biomimetics*, 10(2):026003, 2015.

[5] L. Fraundorfer, F.and Heng, D. Honegger, G. H. Lee, L. Meier, P. Tanskanen, and M. Pollefeys. Vision-based autonomous mapping and exploration using a quadrotor mav. In *Intelligent Robots and Systems (IROS), 2012 IEEE/RSJ International Conference on*, pages 4557–4564. IEEE, 2012.

[6] G. Arleo, F. Caccavale, G. Muscio, and F. Pierri. Control of quadrotor aerial vehicles equipped with a robotic arm. In *Control & Automation (MED), 2013 21st Mediterranean Conference on*, pages 1174–1180. IEEE, 2013.

[7] S. Kim, S. Choi, and H. J. Kim. Aerial manipulation using a quadrotor with a two dof robotic arm. In *Intelligent Robots and Systems (IROS), 2013 IEEE/RSJ International Conference on*, pages 4990–4995. IEEE, 2013.

[8] B. Yüksel, C. Secchi, H. H. Bülthoff, and A. Franchi. Reshaping the physical properties of a quadrotor through ida-pbc and its application to aerial physical interaction. In *Robotics and Automation (ICRA), 2014 IEEE International Conference on*, pages 6258–6265. IEEE, 2014.

[9] A. Albers, S. Trautmann, T. Howard, T. A. Nguyen, M. Frietsch, and C. Sauter. Semi-autonomous flying robot for physical interaction with environment. In *Robotics Automation and Mechatronics (RAM), 2010 IEEE Conference on*, pages 441–446. IEEE, 2010.

[10] L. Marconi and R. Naldi. Control of aerial robots: Hybrid force and position feedback for a ducted fan. *IEEE Control Systems*, 32(4):43–65, 2012.

[11] G. Darivianakis, K. Alexis, M. Burri, and R. Siegwart. Hybrid predictive control for aerial robotic physical interaction towards inspection operations. In *Robotics and Automation (ICRA), 2014 IEEE International Conference on*, pages 53–58. IEEE, 2014.

[12] A. Briod, P. Kornatowski, J. C. Zufferey, and D. Floreano. A collision-resilient flying robot. *Journal of Field Robotics*, 31(4):496–509, 2014.

[13] Dexin Wang and Yuting Rui. Simulation of the stick-slip friction between steering shafts using adams/pre. In *Proc. of the Int. ADAMS User Conference*. Citeseer, 2000.

[14] Z. Cai, M. S. de Queiroz, and D. M. Dawson. A sufficiently smooth projection operator. *IEEE Transactions on Automatic Control*, 51(1):135–139, 2006.